environmental microbiology

Environmental Microbiology (2022) **24**(9), 4437–4448 doi:10.1111/1462-2920.16075

The carnitine degradation pathway of *Acinetobacter baumannii* and its role in virulence

Jennifer Breisch,[1] Clemens Schumm,[1] Anja Poehlein,[2] Rolf Daniel[2] and Beate Averhoff[1*]

[1]*Department of Molecular Microbiology & Bioenergetics, Institute of Molecular Biosciences, Goethe-University Frankfurt am Main, Frankfurt, Germany.*

[2]*Department of Genomic and Applied Microbiology and Göttingen Genomics Laboratory, Institute of Microbiology and Genetics, Georg-August University of Göttingen, Göttingen, Germany.*

Summary

The opportunistic human pathogen *Acinetobacter baumannii* can grow with carnitine but its metabolism, regulation and role in virulence remained elusive. Recently, we identified a carnitine transporter encoded by a gene closely associated with potential carnitine degradation genes. Among those is a gene coding for a putative D-malate dehydrogenase (Mdh). Deletion of the *mdh* gene led to a loss of growth with carnitine but not L-malate; growth with D-malate was strongly reduced. Therefore, it is hypothesized that D-malate is formed during carnitine oxidation and further oxidized to CO_2 and pyruvate and, that not, as previously suggested, L-malate is the product and funnelled directly into the TCA cycle. Mutant analyses revealed that the hydrolase in this cluster funnels acetylcarnitine into the degradation pathway by deacetylation. A transcriptional regulator CarR bound in a concentration-dependent manner to the intergenic region between the *mdh* gene, the first gene of the carnitine catabolic operon and the *carR* gene in the presence and absence of carnitine. Both carnitine and D-malate induced CarR-dependent expression of the carnitine operon. Infection studies with *Galleria mellonella* larvae demonstrated a strong increase in virulence by addition of carnitine indicating that carnitine degradation plays a pivotal role in virulence of *A. baumannii*.

Received 30 March, 2022; revised 10 May, 2022; accepted 16 May, 2022. *For correspondence. E-mail averhoff@bio.uni-frankfurt.de. Tel. +49 69 79829509; Fax +49-69-798-29306.

Introduction

Acinetobacter baumannii is an opportunistic human pathogen which has become an emerging threat in healthcare institutions due to increasing antibiotic resistances (Villegas and Hartstein, 2003; Antunes *et al*., 2014; Harding *et al*., 2018). The success of *A. baumannii* in the hospital environment is based on its outstanding desiccation resistance and persistence in the human host (Dijkshoorn *et al*., 1987; Wendt *et al*., 1997; Peleg *et al*., 2008; Towner, 2009; Zeidler and Müller, 2019). The latter is fostered by its ability to metabolize host-derived carbon and nitrogen sources, allowing survival and thriving in different host niches such as lungs (pneumonia), blood, urinary tract or wounds (Dijkshoorn *et al*., 2007; Fiester and Actis, 2013). Host-derived carbon sources which are metabolized by *A. baumannii* and therefore are good candidates to play a role in metabolic adaptation are sugars, alcohols, lipids, amino acids, organic acids, aromatic compounds and quaternary amines, such as carnitine and choline (Camarena *et al*., 2010; Stahl *et al*., 2015; Breisch *et al*., 2018; Hubloher *et al*., 2020; König *et al*., 2021). The latter are very abundant in human hosts such as choline is the head group moiety of phosphatidylcholine (PC) and sphingomyelin which form 50%–90% of the phospholipids in the outer leaflet of eukaryotic plasma membranes (Zachowski, 1993). Especially the membranes of lung epithelial cells are choline rich and consist of up to 70% PC (Keller and Ladda, 1979). Carnitine is also very abundant in human host tissues and is found in blood, liver, kidney, brain and heart. Carnitine plays a primary role in the carnitine shuttle in mitochondria where it transports long-chain fatty acids for subsequent fatty acid β-oxidation (Bernal *et al*., 2007; McCann *et al*., 2021).

The quaternary amine L-carnitine (hereafter referred to as 'carnitine') is used by *A. baumannii* as carbon and energy source (Zhu *et al*., 2014; Breisch *et al*., 2018). Recently, we identified a betaine/choline/carnitine transporter, Aci01347, which mediates the energy-dependent uptake of carnitine but also choline by *A. baumannii* ATCC 19606 (Breisch *et al*., 2018). Further studies revealed that Aci01347 is not activated by osmolarity which is consistent with our suggestion that carnitine is used as

carbon and energy source (Breisch *et al*., 2018). The *aci01347* gene is closely associated with a potential carnitine catabolic gene cluster. This gene cluster was previously detected by genome mining for carnitine-degrading enzymes in the genome of *Acinetobacter* ssp. within a human microbiome project (HMP) (Zhu *et al*., 2014). Two genes of this gene cluster, *cntA* and *cntB*, were found to encode a two-component Rieske-type oxygenase/reductase complex (CntAB) which catalyses the degradation of carnitine to trimethylamine (TMA) and malic semialdehyde (Zhu *et al*., 2014; Massmig *et al*., 2020). The reaction mechanism of the CntAB complex was elucidated recently (Massmig *et al*., 2020). The generated malic semialdehyde was suggested to be reduced by a malic semialdehyde dehydrogenase to malate which is suggested to be funnelled into the tricarboxylic acid cycle *via* a malate dehydrogenase (Zhu *et al*., 2014). However, it has to be noted that so far there is no experimental evidence for this pathway except for the CntAB mediated oxidation of carnitine. The malate dehydrogenase gene is preceded by an oppositely orientated potential LysR-type transcriptional regulator (LTTR) gene, which is a good candidate to mediate transcriptional regulation of the carnitine catabolic gene cluster (Zhu *et al*., 2014; Breisch *et al*., 2018).

In this study we identified an acetylcarnitine hydrolase (Hyd) in *A. baumannii* ATCC 19606 mediating the conversion of acetylcarnitine to carnitine. Carnitine is further oxidized to D-malate. In contrast to the expectations, D-malate is further decarboxylated to pyruvate and CO_2, catalysed by a malate dehydrogenase (Mdh) encoded by the first gene of the carnitine degradation cluster. Furthermore, we identified an LTTR acting as activator of the carnitine degradation pathway in the presence of the inducer substrates carnitine, D-malate and acetylcarnitine. We show that the genes of the carnitine catabolic pathway form an operon and that the transcriptional regulator CarR binds to the intergenic DNA region between *mdh* and *carR*. Moreover, we provide evidence by *Galleria mellonella* larvae infection studies that the carnitine degradation pathway plays a role in virulence.

Experimental procedures

Bacterial strains and culture conditions

Escherichia coli BL21 STAR was grown in LB medium (Bertani, 1951) at 37°C in the presence of 100 μg ml^{-1} ampicillin. *Acinetobacter baumannii* strains were grown at 37°C in LB medium (Bertani, 1951) or in mineral medium that consists of 50 mM phosphate buffer, pH 6.8, and different salts (Zeidler *et al*., 2017) and 20 mM of acetate, carnitine, acetylcarnitine or D-malate were used as carbon source. 50 μg ml^{-1} kanamycin was added when appropriate. The growth experiments were repeated three times and the ±S.E.M. is shown. Growth curves were fitted manually.

Markerless mutagenesis of A. baumannii ATCC 19606

To generate *Δhyd*, *Δmdh* and *ΔcarR* mutants, 1500 bp upstream and 1500 bp downstream of the genes were amplified from *A. baumannii* ATCC 19606 genomic DNA (primer pairs: Suppl. Table 1) and cloned in pBIISK_*sacB*/*kanR* (Stahl *et al*., 2015) using NotI and PstI. Plasmid was transformed in electrocompetent *A. baumannii* wild type cells. Electrocompetent *A. baumannii* cells were prepared as described before (Stahl *et al*., 2015). Electroporation was performed at 2.5 kV, 200 Ω and 25 μF. Transformants were selected on LB agar using 50 μg ml^{-1} kanamycin and verified by PCR (primer pairs: Suppl. Table 1). Segregation was induced by counter selection using 10% sucrose for 18 h at 37°C followed by plating on LB agar containing 10% sucrose. Single colonies exhibiting kanamycin sensitivity were verified by PCR (primer pairs: Suppl. Table 1).

RNA isolation, cDNA synthesis and bridging PCR

For RNA isolation cells were grown overnight in mineral medium with 20 mM carnitine as carbon source. 5 ml of cell cultures were harvested in the stationary phase by centrifugation (10 min, 4°C, 4700 rpm) and re-suspended in 2 ml Tri-Reagent® (Sigma-Aldrich). After 15 min of incubation at room temperature, 0.2 ml chloroform was added, mixed, and followed by incubation for 15 min at room temperature and centrifugation (15 min, 4°C, 12 000*g*). The aqueous phase was transferred to a new reaction tube. After addition of 500 μl isopropanol to the aqueous phase and 10 min incubation at room temperature, nucleic acids were precipitated by centrifugation (10 min, 4°C, 12 000*g*) and re-suspended in 50 μl H_2O. Subsequently, DNA contaminations were removed by digestion with TURBO™ DNase (Invitrogen) and proteins were removed by repeating chloroform treatment described above. RNA was used for reverse transcription using M-MLV Reverse Transcriptase (Promega). For bridging PCR analyses 100 ng of cDNA, DNase digested RNA or genomic DNA was used as templates and Phusion DNA-Polymerase (NEB) for amplification. The resulting PCR products were analysed by agarose gel electrophoresis.

RNA extraction and RNA sequencing

To perform RNA extraction for transcriptomic analysis cells were grown to an OD_{600} of 0.5 in mineral medium with 20 mM carnitine, acetylcarnitine, D-malate or

succinate as carbon source and 2 ml of the cultures were harvested by centrifugation (10 min, 4°C, 4700 rpm). Harvested cells were re-suspended in 800 µl RLT buffer (RNeasy Mini Kit, Qiagen) with β-mercaptoethanol (10 µl ml^{-1}) and cell lysis was performed using a laboratory ball mill. Subsequently, 400 µl RLT buffer (RNeasy Mini Kit Qiagen) with β-mercaptoethanol (10 µl ml^{-1}) and 1200 µl 96% (vol./vol.) ethanol were added. For RNA isolation, the RNeasy Mini Kit (Qiagen) was used as recommended by the manufacturer, but instead of RW1 buffer RWT buffer (Qiagen) was used in order to isolate RNAs smaller than 200 nucleotides also. To determine the RNA integrity number the isolated RNA was run on an Agilent Bioanalyzer 2100 using an Agilent RNA 6000 Nano Kit as recommended by the manufacturer (Agilent Technologies, Waldbronn, Germany). Remaining genomic DNA was removed by digesting with TURBO DNase (Invitrogen, Thermo Fischer Scientific, Paisley, UK). The Pan-Prokaryotes riboPOOL kit v4 (siTOOLS BIOTECH, Planegg/Martinsried, Germany) was used to reduce the amount of rRNA-derived sequences (samples 1–3) and the Illumina Ribo-Zero plus rRNA Depletion Kit (Illumina, San Diego, CA, USA) was used to reduce the amount of rRNA-derived sequences of samples 4–12. For sequencing, the strand-specific cDNA libraries were constructed with a NEBNext Ultra II Directional RNA library preparation kit for Illumina and the NEBNext Multiplex Oligos for Illumina (96) (New England BioLabs, Frankfurt am Main, Germany). To assess quality and size of the libraries samples were run on an Agilent Bioanalyzer 2100 using an Agilent High Sensitivity DNA Kit as recommended by the manufacturer (Agilent Technologies). Concentration of the libraries was determined using the Qubit® dsDNA HS Assay Kit as recommended by the manufacturer (Life Technologies GmbH, Darmstadt, Germany). Sequencing of samples 1–3 was performed on the HiSeq4000 instrument (Illumina) using HiSeq® 3000/4000 SBS Kit (50 cycles) and the HiSeq 3000/4000 SR Cluster Kit (Illumina) in single-end mode with 50 bp read length. For sequencing of samples 4–12 the NovaSeq 6000 instrument (Illumina) with the NovaSeq 6000 SP Reagent Kit v1.5 (100 cycles) and the NovaSeq XP 2-Lane Kit v1.5 was used in the paired-end mode and 2× 50 cycles. For quality filtering and removing of remaining adaptor sequences, Trimmomatic-0.39 (Bolger *et al*., 2014) and a cutoff phred-33 score of 15 were used. The mapping against the reference genomes of *A. baumannii* ATCC 19606 (Ref: NZ_CP058289.1) was performed with Salmon (v 1.5.2) (Patro *et al*., 2017). As mapping backbone a file that contains all annotated transcripts excluding rRNA genes and the whole genome of the references as decoy was prepared with a k-mer size of 11. Decoy-aware mapping was done in selective-alignment mode with '–mimicBT2', '–disableChainingHeuristic' and '–recoverOrphans' flags as well as sequence and position bias correction and 10 000 bootstraps. For –fldMean and –fldSD, values of 325 and 25 were used respectively. The quant.sf files produced by Salmon were subsequently loaded into R (v 4.0.5) (R Core Team, 2020) using the tximport package (v 1.18.0) (Soneson *et al*., 2015). DeSeq2 (v 1.30.0) (Love *et al*., 2014) was used for normalization of the reads and fold change shrinkages were also calculated with DeSeq2 and the apeglm package (v 1.12.0) (Zhu *et al*., 2019). Genes with a log2-fold change of $+5/-5$ and a *p*-adjust value <0.05 were considered differentially expressed. Raw reads have been deposited in the Sequence Read Archive as BioProject PRJNA821016.

Cloning, expression and purification of CarR

To express *carR* in *E. coli* BL21 STAR, the gene was cloned into the multiple cloning site of pBAD/HisA using EcoRI and PstI (primer pairs in Suppl. Table 1).

E. coli BL21 STAR harbouring plasmid pBAD/HisA_*carR* was used to inoculate 1 L of LB medium containing 100 µg ml^{-1} ampicillin. After reaching an OD_{600} of 0.7–0.8 gene expression was induced for 3 h by addition of IPTG to a final concentration of 1 mM, cells were harvested by centrifugation (8000*g* for 7 min at 4°C), washed in 50 ml lysis buffer (50 mM Tris, 300 mM NaCl, 10 mM imidazole, pH 8,0) and stored at −20°C.

For purification of CarR, frozen cells were thawed on ice, re-suspended in 15 ml lysis buffer containing DNase and 0.5 mM PMSF and disrupted via French Press (three times, 1000 psi). Cell debris was removed (14 000*g*, 30 min, 4°C) and cell-free lysate was incubated with 1 ml of Ni-NTA material for 30 min and shaken at 4°C for binding of His-CarR to the Ni-NTA matrix. Column was washed with 10 ml washing buffer 1 (50 mM Tris, 300 mM NaCl, 50 mM imidazole, pH 8.0), 10 ml washing buffer 2 (50 mM Tris, 300 mM NaCl, 70 mM imidazole, pH 8.0) and elution of CarR was performed using 10 ml elution buffer in 1 ml elution steps (50 mM Tris, 300 mM NaCl, 150 mM imidazole, pH 8.0). The protein concentration was determined by Bradford (1976). Protein composition of the different fractions was analysed by electrophoresis through a 12.5% sodium dodecyl sulfate-polyacrylamide gel according to Laemmli (1970) stained with Coomassie (0.5 g L^{-1} Serva Blue R-250, 100 ml L^{-1} methanol, 100 ml L^{-1} glacial acetic acid).

Electrophoretic mobility shift assay

For the EMSA studies, the regulator CarR was expressed and produced in *E. coli* BL21 STAR cells and purified. The DNA fragments used in the EMSA studies were amplified by PCR using the primer pairs given in the

Suppl. Table 1. 233 fmol of the 693 bp fragment spanning the intergenic region between the *carR* and *mdh* gene and a non-related 1613 bp DNA fragment were incubated with 0–81 pmol of CarR in a total volume of 20 µl with 1× EMSA reaction buffer [10 mM Tris, 1 mM EDTA, 0.1 mM KCl, 5% (vol./vol.) glycerin, pH 8.0] for 30 min at room temperature. 2 µl of EMSA loading dye [10 mM Tris, 1 mM EDTA, 100 mM KCl, 50% (vol./vol.) glycerin, bromphenolic blue, xylene cyanol, pH 8,0] was added to the reaction and 20 µl was analysed by native polyacrylamide electrophoresis.

Galleria mellonella *infection studies*

Caterpillars (provided by a local provider) were preselected by melanization, size (400 ±50 mg) and movement in response to touch. *A. baumannii* wild type and mutants were grown in LB until an OD_{600} of 1.0–1.5, harvested (10 min, 4700 rpm), washed with phosphate-buffered saline (2.7 mM KCl, 1.5 mM KH_2PO_4, 137.9 mM NaCl, 8.1 mM Na_2HPO_4) and adjusted to a final OD_{600} of 1.5. Twenty caterpillars were used per experiment and per strain. 10 µl (~6 × 10^6 CFU) of the cell suspension was injected into the last prolegs. As control 10 untreated caterpillars as well as 20 caterpillars were treated with 10 µl of PBS, 10 µl of PBS with 5 mM carnitine, acetylcarnitine, D-malate or acetate. Caterpillars were incubated at 37°C for 5 days and survival was documented every 24 h. All experiments were repeated at least three times and the ±S.E.M. was shown. Significance of survival differences was assessed by *t*-test.

Results

Characterization of the carnitine degradation gene cluster

Recently, we identified a secondary transporter Aci01347 mediating carnitine uptake of *A. baumannii*. The transporter gene is located in a gene cluster comprising Rieske-type oxygenase/reductase (*cntAB*) genes and other genes suggested to play a role in carnitine metabolism (Fig. 1A) (Zhu *et al*., 2014; Breisch *et al*., 2018). Upstream of the transporter gene *aci01347* is an open reading frame coding for a 370 amino acid protein annotated as malate dehydrogenase (Mdh). This protein shares high amino acid sequence similarities and identities with the tartrate dehydrogenase of *Pseudomonas putida* (90% similarity/70% identity) and the D-malic enzyme of *Rhodobacter capsulatus* (90% similarity/72% identity), which are responsible for the oxidative decarboxylation of tartrate to oxaloglycolate and D-malate to pyruvate respectively (Tipton and Peisach, 1990; Martínez-Luque *et al*., 2001). Upstream of this gene is in opposite orientation a gene coding for a potential LTTR comprising 326 amino acids. This LTTR is 76.8% similar and 46.4% identical to the LTTR of *E. coli* O157:H7, which is a transcriptional activator of a D-malate dehydrogenase (Lukas *et al*., 2010). The open reading frame downstream of *aci01347* encodes a 324 amino acid predicted hydrolase (Hyd), which displays highest similarities (62.2%) and identities (41.7%) to a lipolytic protein with unknown function from *Pseudomonas aeruginosa* PAO1. The gene of the putative hydrolase is flanked downstream by the *cntA* gene, which encodes the carnitine oxygenase. The open reading frame downstream of *cntA* encodes a 483 amino acid protein which was predicted to encode a malic semialdehyde dehydrogenase (MsaDH). The deduced protein shows highest amino acid sequence similarities and identities of 87.7% and 61.7% respectively, to a succinate semialdehyde dehydrogenase of *E. coli* O157:H7. The last gene of the carnitine degradation cluster, *cntB*, has already been identified as carnitine reductase subunit of the CntAB complex (Zhu *et al*., 2014; Massmig *et al*., 2020). The finding that CntAB are essential for the conversion of carnitine to TMA together with the similarities of the gene products of closely associated genes (Fig. 1A) suggests that the malic semialdehyde generated by CntAB is further oxidized by the potential MsaDH to malate followed by conversion to pyruvate mediated by a potential Mdh (Fig. 1B). However, it has to be noted that so far only the role of CntAB in carnitine conversion to malic semialdehyde and TMA has been experimentally proven, whereas there is no experimental evidence with respect to the function of other gene products of the carnitine degradation gene cluster. The presence of a potential hydrolase gene (*hyd*) in the carnitine degradation gene cluster led to the hypothesis, that also acetylcarnitine is used as sole carbon and energy source by *A. baumannii*.

Acetylcarnitine and D-malate are degraded via the carnitine catabolic pathway

To analyse the role of *hyd* and *mdh* in carnitine catabolism markerless *Δhyd* and *Δmdh* mutants of *A. baumannii* were generated using a kanamycin resistance cassette (*kanR*) as positive selection marker and a levansucrase (*sacB*) for counter selection on sucrose. The deletion mutants were verified by sequencing. The *Δhyd* mutant was completely defective in growth with acetylcarnitine as sole carbon and energy source (Fig. 2B), whereas growth with acetate was unaffected (Fig. 2A). The *Δhyd* mutant was still able to grow with carnitine and exhibited a growth rate of 0.45 h^{-1} comparable to the growth rate of the wild type (0.56 h^{-1}; Fig. 2C). However, the *Δhyd* mutant exhibited a prolonged lag phase of 14 h in comparison to the wild type cells which entered the

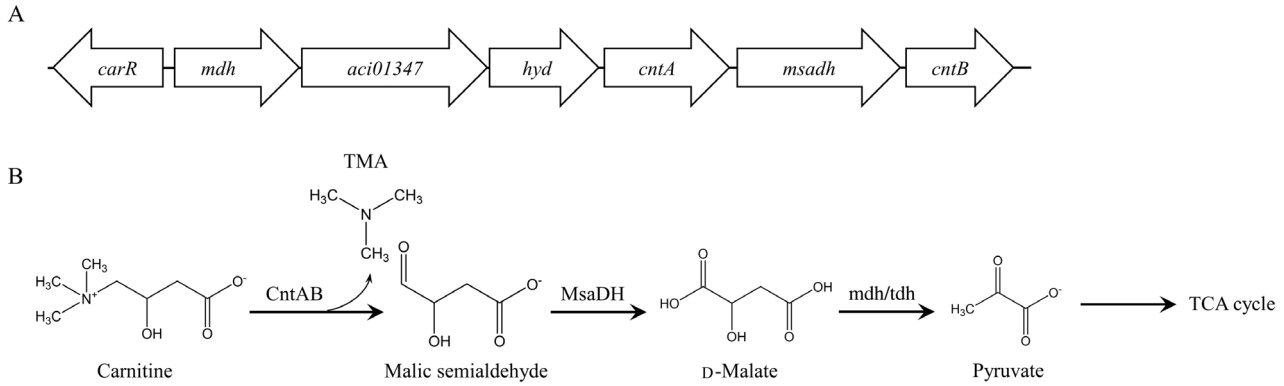

Fig. 1. Organization of the putative carnitine degradation gene cluster (A) and predicted pathway of carnitine and acetylcarnitine degradation (B). A. Organization of the carnitine degradation cluster (*carR*: LysR-type transcriptional regulator; *mdh*: malate dehydrogenase; *aci01347*: carnitine transporter; *hyd*: acetylcarnitine hydrolase; *cntA* and *cntB*: Rieske-type oxidoreductase complex; *msadh*: malic semialdehyde dehydrogenase). B. Acetylcarnitine is suggested to be converted by the putative hydrolase Hyd to carnitine, which is further degraded by the CntAB complex to malic semialdehyde and TMA. Malic semialdehyde is suggested to be metabolized to malate by the malic semialdehyde dehydrogenase MsaDH followed by the conversion to pyruvate and CO_2 mediated by the putative malate dehydrogenase Mdh.

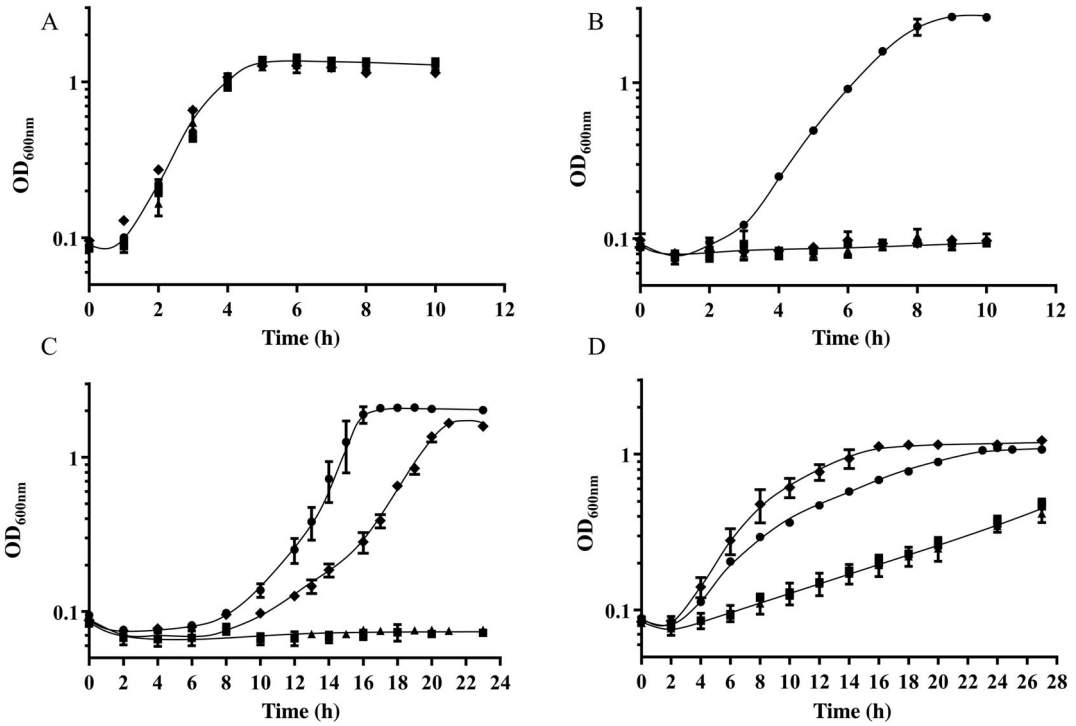

Fig. 2. Growth studies of the *A. baumannii* ATCC 19606 wild type and the *Δmdh*, *Δhyd* and *ΔcarR* mutants in mineral medium with acetate, acetylcarnitine, carnitine or D-malate as sole carbon and energy source. *A. baumannii* ATCC 19606 wild type cells (●), *Δhyd* (◆), *Δmdh* (■) and *ΔcarR* mutants (▲) were grown in mineral medium with 20 mM acetate (A), 20 mM acetylcarnitine (B), 20 mM carnitine (C) or 20 mM D-malate (D) as sole carbon and energy source. Each value is the mean of ±S.E.M. of at least three independent measurements. The curves were fitted manually.

exponential growth phase after 10 h of growth. The *Δhyd* mutant exhibited a slightly increased growth rate (0.29 h^{-1}) with D-malate (Fig. 2D) in comparison to the wild type (0.22 h^{-1}). Taken together these studies led to the conclusion that *hyd* encodes an acetylcarnitine hydrolase essential for the conversion of acetylcarnitine to carnitine.

Growth experiments with the *Δmdh* mutant revealed that this mutant was completely defective in growth with acetylcarnitine (Fig. 2B) or carnitine (Fig. 2C) as sole carbon source, whereas growth with acetate was not affected (Fig. 2A). Moreover, the *Δmdh* mutant exhibited a significantly decreased growth rate with D-malate (0.08

h^{-1}) in comparison to the wild type (0.22 h^{-1}). The *Δmdh* mutant was unaffected in growth with L-malate as expected due to the presence of an L-malate dehydrogenase in the TCA cycle (data not shown). The impaired growth of the *Δmdh* mutant with D-malate together with the significant similarities and identities of the Mdh to the D-malic enzyme of *R. capsulatus* led to the conclusion that *mdh* encodes a D-malate dehydrogenase essential for the conversion of D-malate to pyruvate plus CO_2, the last step in carnitine catabolism (Tipton and Peisach, 1990; Martínez-Luque *et al*., 2001). The slow growth of the *Δmdh* mutant with D-malate as sole carbon source could be due to the presence of racemases leading to the conversion of D-malate to L-malate which can be oxidized via the L-malate dehydrogenase of the TCA cycle.

CarR is an activator of carnitine catabolism

The close association of a potential LTTR gene (*carR*) suggests a role of this potential regulator in transcriptional regulation of the carnitine gene cluster. To get insights into the role of CarR in regulation of the carnitine degradation pathway, a *ΔcarR* mutant was generated using the *sacB* system. The *ΔcarR* mutant was verified by sequencing. The *ΔcarR* mutant was completely defective in growth with acetylcarnitine (Fig. 2B) or carnitine (Fig. 2C), whereas growth with acetate was unaffected (Fig. 2A). Growth with D-malate was not completely abolished (Fig. 2D) but the growth rate was significantly reduced to 0.06 h^{-1} comparable to the reduced growth rate of the *Δmdh* mutant. The growth defect of the *ΔcarR* mutant suggests that CarR is the transcriptional activator of the carnitine degradation cluster.

Genes of the carnitine catabolism pathway are organized in an operon

Next, we addressed the transcriptional organization of the carnitine degradation gene cluster by bridging PCR. Therefore, cDNA was used as template synthesized from RNA extracted from carnitine induced *A. baumannii* cells and primers were used that span the different open reading frames (Suppl. Table 1). The amplified intergenic regions are indicated in Fig. 3A and the detection of the amplified PCR products *via* agarose gel electrophoresis is shown in Fig. 3B. The results obtained demonstrate that *mdh*, *aci01347*, *hyd*, *cntA*, *msadh* and *cntB* form an operon. Control experiments showed that RNA was free from contamination with genomic DNA. No amplification of the intergenic region was observed in the absence of reverse transcriptase and in the absence of template. Furthermore, amplification of the intergenic region between *mdh* and *carR* and of the intergenic region between *carR* and the upstream located open reading frame HMPREF0010_01344 only led to PCR products with genomic DNA as template. Same holds true for the intergenic region between the *cntB* gene and HMPREF0010_01352. These findings led to the conclusion that the open reading frames HMPREF0010_01344 and HMPREF0010_01352 as well as the *carR* gene are not part of the operon of the carnitine catabolic pathway.

Acetylcarnitine, carnitine and D-malate induced transcription of the carnitine operon

To get insights into the transcriptional regulation of the carnitine catabolic pathway we cultivated *A. baumannii* with acetylcarnitine, carnitine, D-malate and succinate as sole carbon and energy source respectively. Genome-wide expression profiling was performed using RNA isolated from cultures grown with these different substrates. These analyses revealed that genes of the carnitine degradation pathway were upregulated in the presence of acetylcarnitine, carnitine as well as D-malate by a $\log_2$-fold change of 4.86–8.87 (Suppl. Table 2). Moreover, the transcriptome analyses revealed that the carnitine operon is transcribed at a basal level also under non-inducing conditions with succinate as carbon source; transcript numbers of 50–500 were detected for the genes of the carnitine catabolic pathway (*aci01347*: 371 ∓ 11, *hyd*: 559 ∓ 14, *cntA*: 420 ∓ 7, *cntB*: 275 ∓ 22, *carR*: 94 ∓ 12, *mdh*: 59 ∓ 2). The basal transcript levels guarantee a very fast adaptation upon availability of the inducer substrates. Interestingly, several genes not obviously linked to carnitine degradation were also significantly upregulated after growth with acetylcarnitine, carnitine or D-malate. One such upregulated gene cluster encodes potential key enzymes for degradation of aromatic compounds *via* the phenylacetic acid pathway or the homogentisate pathway (Suppl. Table 2). The latter is the central catabolic pathway for the degradation of L-phenylalanine and L-tyrosine. Moreover, several genes are significantly downregulated under these conditions, such as ribosomal genes, cold shock protein genes and many hypothetical proteins (Suppl. Table 3).

CarR binds constitutively to the intergenic DNA region between mdh and carR

Next, we analysed whether CarR binds to the intergenic DNA region between the first gene (*mdh*) of the carnitine operon and the *carR* gene and addressed the question of whether DNA binding is inducer substrate-dependent. To this end, electromobility shift assays (EMSA) were performed. Therefore, the regulator gene was cloned with an N-terminal His_6-Tag into the expression vector pBAD/

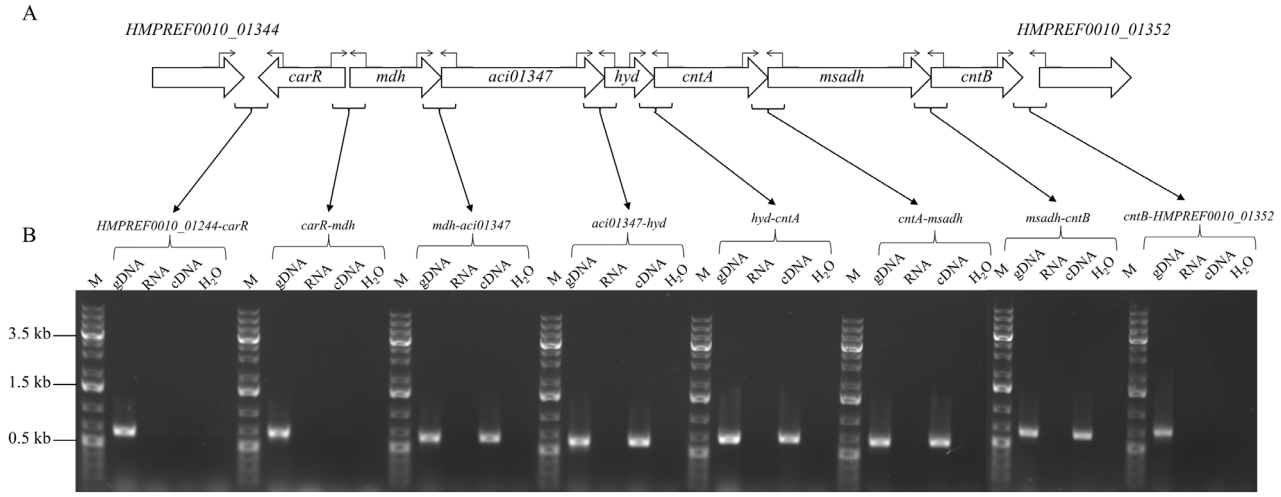

Fig. 3. The genes of the carnitine degradation pathway form an operon.
(A) Intergenic regions amplified by bridging PCRs. The intergenic regions are indicated by clamps below the genes and arrows above the genes indicate primer binding sites. Arrows indicate the related PCR analysis. The open reading frames upstream and downstream of the carnitine degradation cluster are designated with HMPREF0010_01344 and HMPREF0010_01352 respectively.
(B) Electrophoretic analysis of the PCR products from the bridging PCRs. PCR products of the PCRs with genomic DNA as template are labelled with 'gDNA', those with cDNA as template are labelled with 'cDNA', those with RNA as template are labelled with 'RNA' and those without template are labelled with 'H_2O'. 200 ng of PCR products were separated in a 0.8% (wt./vol.) agarose gel and the 100 bp DNA-ladder (Thermo Fisher) was used as marker.

HisA (Suppl. Fig. 1A) and His_6-CarR was produced in *E. coli* BL21 STAR cells and purified via Ni-NTA affinity chromatography. The deduced mass of the purified protein corresponds to the deduced molecular mass of CarR of 37.03 kDa (Suppl. Fig. 1B). Furthermore, the entire intergenic DNA region between *carR* and *mdh* plus 292 bp of the 5′ end of *carR* and 298 bp of the 5′ end of *mdh* was amplified *via* PCR (primer pair in Suppl. Table 1). Next, we addressed whether CarR binds to the 693 bp DNA fragment and indeed, preincubation of purified His_6-CarR resulted in a mobility shift (Fig. 4). Three different protein–DNA complexes were detected and designated complex 1, complex 2 and complex 3 (Fig. 4).

Next, we analysed whether the inducer substrates carnitine and D-malate influence the binding of CarR to the DNA. These studies revealed that preincubation with carnitine or D-malate led to the same complexes as observed in the absence of inducer substrates (data not shown). These data indicate that the transcriptional regulator of the carnitine degradation operon CarR binds to the DNA independently of the presence of the inducer substrates. Binding specificity was analysed using the 693 bp fragment and an excess of BSA instead of CarR and by using a 1613 bp DNA fragment not linked to the carnitine operon for binding studies with CarR. In both cases no shift of the DNA fragments was observed. These results led to the conclusion that binding of CarR to the intergenic region between *carR* and *mdh* is specific.

Carnitine degradation plays an important role in infection of G. mellonella larvae

Next, we addressed the role of carnitine metabolism in virulence of *A. baumannii* by performing *G. mellonella* caterpillar infection studies with the *A. baumannii* ATCC 19606 wild type and the *ΔcarR* mutant in the absence (Fig. 5A) and in the presence (Fig. 5B) of carnitine. In the absence of carnitine, no difference in virulence of the wild type and the *ΔcarR* mutant was observed, the survival of the *G. mellonella* larvae after infection with the wild type or the *ΔcarR* mutant was comparable over 5 days (Fig. 5A). In the presence of carnitine during infection of the *G. mellonella* caterpillars a significant ($p \leq 0.05$) increase in virulence was observed for the wild type cells (Fig. 5B), such as after one day only 25% of the infected caterpillars died in the absence of carnitine (Fig. 5A), and 75% of the larvae died after infection with wild type cell suspensions in PBS with 5 mM carnitine (Fig. 5B). In contrast, the *ΔcarR* mutant exhibited a significantly ($p \leq 0.05$) lower virulence in the presence of carnitine in comparison to the wild type cells, such as the survival of *G. mellonella* after infection with *ΔcarR* mutant in the presence of carnitine was comparable to the survival in the absence of carnitine. Here, 60% of the larvae with *ΔcarR* injection survived after 1 day in the presence of carnitine and 75% in the absence of carnitine. These results suggest that carnitine degradation plays an important role in virulence of *A. baumannii*.

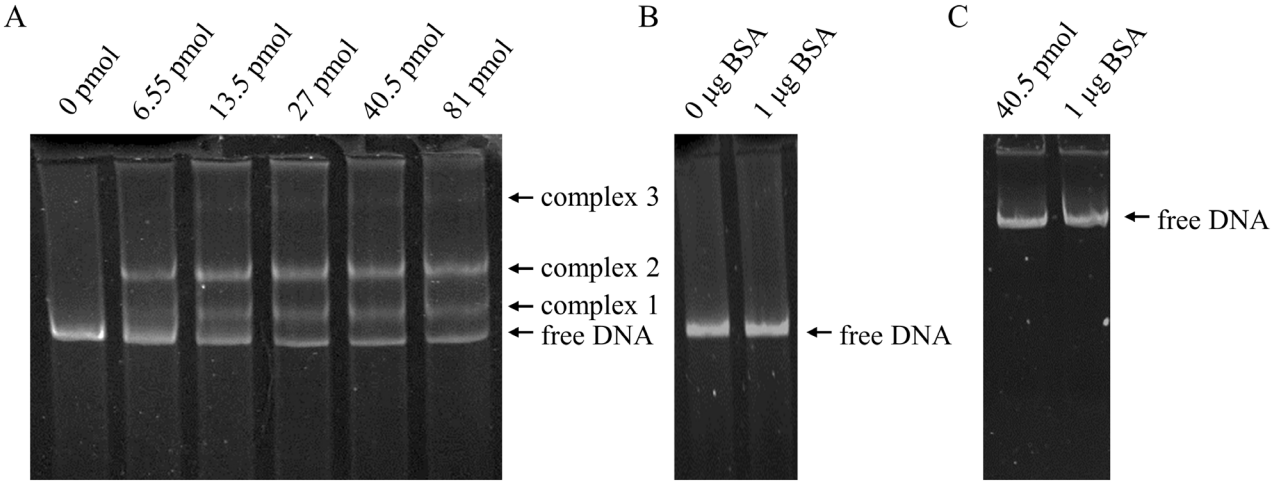

Fig. 4. CarR binds to a 693 bp DNA fragment spanning the intergenic region between *mdh* and *carR*.
(A) Binding of CarR to a 693 bp DNA fragment upstream of the carnitine degradation operon was analysed by EMSA studies. Different amounts of protein (0–81 pmol CarR) were incubated for 30 min with 233 fmol of the DNA fragment followed by separation on a 5% (vol./vol.) native polyacrylamide gel. DNA was visualized with ethidium bromide.
(B) The shift of the 693 bp DNA fragment spanning the intergenic region between *mdh* and *carR* was analysed in the presence or absence of 1 µg BSA to verify specificity of binding. 1 µg BSA was incubated for 30 min with 233 fmol of the DNA fragment followed by separation on a 5% (vol./vol.) native polyacrylamide gel. DNA was visualized with ethidium bromide.
(C) Binding of CarR to a non-specific DNA fragment was analysed with 233 fmol of a 1613 bp DNA fragment. The DNA was incubated for 30 min with 40.5 pmol CarR or 1 µg BSA followed by separation on a 5% (vol./vol.) native polyacrylamide gel. DNA was visualized with ethidium bromide.

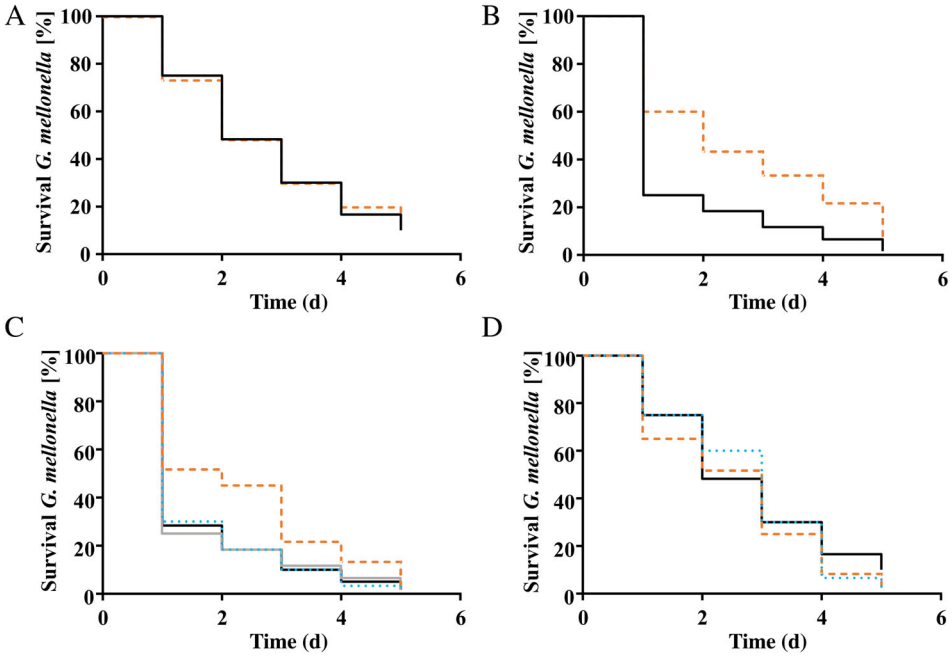

Fig. 5. Carnitine and acetylcarnitine degradation of *A. baumannii* plays a role in *G. mellonella* infection. Survival of *G. mellonella* caterpillars after infection with (A) the wild type (black solid line) or the *ΔcarR* mutant (orange dashed line) in the absence of carnitine or acetylcarnitine. (B) The wild type (black solid line) or the *ΔcarR* mutant (orange dashed line) in the presence of 5 mM carnitine. (C) The wild type or the *Δhyd* mutant in the presence of 5 mM acetylcarnitine or 5 mM carnitine (wild type with carnitine: grey solid line; wild type with acetylcarnitine: black solid line; *Δhyd* with carnitine: blue dotted line; *Δhyd* with acetylcarnitine: orange dashed line). (D) The wild type in the absence (black solid line) or in the presence of 5 mM acetate (blue dotted line) or 5 mM D-malate (orange dashed line). Wild type, *ΔcarR* and *Δhyd* cells were grown to stationary growth phase in LB, harvested and washed three times in sterile PBS and finally re-suspended to an OD_{600} of 1.5 in PBS, PBS with 5 mM carnitine or PBS with 5 mM acetylcarnitine. 10 µl (~1×10^6 CFU) was injected into each *G. mellonella* larvae. Pre- and post-selection was performed as described in Experimental procedures. One representative out of at least three experiments is shown.

TMA formation during carnitine catabolism is most likely important for A. baumannii virulence

The increased killing of *G. mellonella* in dependence of carnitine degradation could be due to a toxic effect of the TMA formed during carnitine oxidation. To test this hypothesis, we performed *G. mellonella* infection studies with the A. baumannii ATCC 19606 wild type and the *Δhyd* mutant in the presence of acetylcarnitine (Fig. 5C), the latter was no longer able to convert acetylcarnitine to carnitine and therefore TMA production is abolished. Acetylcarnitine also increased killing of caterpillars, but this was abolished in the *Δhyd* (Fig. 5C). When carnitine was supplied to the *Δhyd* mutant, the effect was restored. These data indicate that metabolism of carnitine or acetylcarnitine is responsible for this effect. Oxidation of both substrates leads to the production of TMA, a potent inhibitor of microbial growth. Degradation of the carnitine pathway intermediate D-malate leads to pyruvate and if indeed TMA production is responsible for the increased killing of *G. mellonella* in the presence of carnitine or acetylcarnitine the presence of D-malate during *G. mellonella* infection studies should not lead to this effect. Indeed, the presence of D-malate during infection had no significant effect on survival of *G. mellonella* larvae (Fig. 5D). The same was observed with acetate. Taken together these findings suggest that TMA formation during degradation of carnitine has an effect on the viability of *G. mellonella* larvae. However, further studies are required to provide clear evidence that TMA is causing the increased *G. mellonella* killing.

Discussion

In this study, we have addressed the role of *hyd* and *mdh* in carnitine degradation of *A. baumannii*. We demonstrated that *hyd* mediates the conversion of acetylcarnitine to carnitine and that *mdh* is essential for the conversion of the carnitine pathway intermediate D-malate. D-malate is formed by a carnitine oxidoreductase (CntAB) that produces TMA in addition (Zhu *et al*., 2014). A carnitine degradation pathway *via* malate and TMA was first discovered in the mid-1960s in *Serratia marcescens* and up to now has been only further detected in *Acinetobacter calcoaceticus*, later identified as *A. baumannii* strain (Kleber *et al*., 1977; Ditullio *et al*., 1994; Zhu *et al*., 2014; Meadows and Wargo, 2015).

Our finding that a *Δmdh* mutant is significantly impaired in growth with D-malate together with the 90% similarity of the Mdh to the D-malic enzyme of *R. capsulatus* suggests that the Mdh of *A. baumannii* is decarboxylating D-malate to pyruvate. Enzymes of this superfamily catalyse the oxidation and subsequent decarboxylation of different D-malate-based substrates such as D-malate, L-tartrate, 3-isopropylmalate and D-isocitrate with different specificities with various substrate recognition sites. To date, four different substrate recognition motifs have been identified (Vorobieva *et al*., 2014). The isopropylmalate dehydrogenases (IPMDH) which exhibit highest activities with alkylmalates contain the substrate recognition motif RXGXLLXXR (Miyazaki *et al*., 1993; Dean and Dvorak, 1995; Vorobieva *et al*., 2014), whereas the isocitrate dehydrogenases contains a specific serine instead of glutamate and asparagine instead of lysine (XXSXNXXXR) (Stokke *et al*., 2007; Vorobieva *et al*., 2014). The D-malate/tartrate dehydrogenases (Mdh/Tdh) mediate the conversion of D-malate to pyruvate and CO_2 and of tartrate to dihydroxyfumarate. These Mdh/Tdh enzymes contain the substrate recognition site LXXXLXXXR (Giffhorn and Kuhn, 1983; Martínez-Luque *et al*., 2001; Vorobieva *et al*., 2014). In contrast, members of a subcluster of the malate/tartrate dehydrogenases, the TtuC-like proteins, which mediate the conversion of tartrate and not D-malate contain the substrate-binding site (LXXXRXXXC) (Crouzet and Otten, 1995). The Mdh of *A. baumannii* contains the LXXXLXXXR substrate recognition motif which is consistent with our suggestion that the Mdh from A. baummannii ATCC19606 mediates the conversion of D-malate to pyruvate and CO_2.

The significant similarities of CarR to LTTR and the close association of the *carR* gene with the carnitine catabolic operon made it a good candidate for a regulator of the carnitine catabolic pathway and indeed mutant studies suggest that CarR is the activator of the carnitine catabolic pathway. LTTR have a helix-turn-helix motif at the N-terminus which is important for DNA binding. Such a helix-turn-helix motif is also present (amino acid 7–66) at the N-terminus of CarR (pfam00126). Also characteristic for LTTR is the PBP2_CrgA_like_9 domain at the C-terminus (CDD:176168) (Lu *et al*., 2020), consisting of two typical Rossmann folds connected by a linker region in between, which is necessary for substrate binding and dimerization (Lochowska *et al*., 2001; Ezezika *et al*., 2007). This domain is also present in CarR spanning the amino acid 95–291. Our finding that the transcription of the carnitine operon is dependent on carnitine or D-malate suggests that D-malate and carnitine binding to CarR leads to conformational changes in the CarR proteins affecting the CarR/DNA complexes thereby leading to binding of the RNA polymerase at the promoter of the carnitine operon followed by gene expression (Maddocks and Oyston, 2008).

Carnitine is abundant in the human host, such as 70 mmol is present in a 70 kg adult (Engel and Rebouche, 1984). This abundance of carnitine in the human host makes it a good substrate for pathogenic bacteria, as shown for *P. aeruginosa*, which metabolizes carnitine to glycine betaine and further to pyruvate (Wargo and

Hogan, 2009). This carnitine degradation pathway is linked to virulence such as glycine betaine induces the expression of different virulence factors such as phospholipase C and phosphorylcholine phosphatase (Lisa *et al*., 1994; Lucchesi *et al*., 1995; Wargo *et al*., 2009). Our finding that the presence of carnitine or acetylcarnitine in *G. mellonella* infection studies with *A. baumannii* wild type cells led to significantly decreased survival rates of *G. mellonella* larvae suggests that degradation of carnitine is also linked to virulence. The decreased survival of *G. mellonella* larvae in the presence of carnitine might be due to the production of TMA. This is also supported by our finding that mutants defect in carnitine degradation led to *G. mellonella* larvae survival rates comparable to those after infection with *A. baumannii* in the absence of carnitine. These findings suggest that TMA which is released during carnitine oxidation might be responsible for the decreased survival rates. This is in line with the finding that TMA is a toxic compound for vertebrates such as shown for *Necrophorus orbicollis* (Abbott, 1936). Here, injection of TMA in low concentration led to a rapid death of the insects. Furthermore, it has to be noted that increased TMA production in the human host due to carnitine degradation of infecting *A. baumannii* might also affect the health of the human host since TMA is metabolized in the human liver by an flavin-dependent monooxygenase to TMAO (Miao *et al*., 2015) which was shown to cause prevalent cardiovascular disease and enhance the risk for myocardial infarcts and stroke (Koeth *et al*., 2013). Therefore, it is tempting to speculate that carnitine degradation in the human host might not only contribute to metabolic adaptation and virulence of *A. baumannii* but might also trigger cardiovascular diseases. Recently, we generated gene cluster abundance profiles of different metabolic traits in *Acinetobacter* species and found that the ability to metabolize carnitine occurs inside and outside the *A. calcoaceticus–baumannii* (ACB) complex (Djahanschiri *et al*., 2022). This complex represents a group of closely related human opportunistic pathogens. However, 25 of 31 analysed strains outside the ACB complex exhibiting a carnitine degradation pathway were isolated from infected patients. Moreover, the carnitine cluster is absent in *A. calcoaceticus* which is the only non-pathogenic species in the ACB clade. Taken together, the presence of the carnitine gene cluster correlates well with the pathogenicity of the isolates.

Transcriptomic analyses revealed that growth of *A. baumannii* with carnitine, acetylcarnitine and D-malate led to a significant upregulation of the homogentisate and phenylacetic acid pathway genes. The homogentisate pathway is the key catabolic pathway for degradation of phenylalanine, 3-hydroxyphenylacetate and tyrosine (Arias-Barrau *et al*., 2004). The upregulation of these degradation pathways in the presence of carnitine might promote the adaptation to the human host due to the high abundance of phenylalanine, tyrosine and phenylacetic acid in the host.

Acknowledgements

This study was supported by a grant from the Deutsche Forschungsgemeinschaft through DFG Research Unit FOR2251.

Data Availability

Transcriptome data have been deposited in the National Center for Biotechnology Information's (NCBI) Sequence Read Archive (SRA) as BioProject PRJNA821016. All other data of this study are available from the corresponding author upon reasonable request.

References

Abbott, C.E. (1936) The toxicity of trimethylamine for *Necrophorus orbicollis*. *Psyche* **43**: 37–39.

Antunes, L.C., Visca, P., and Towner, K.J. (2014) *Acinetobacter baumannii*: evolution of a global pathogen. *Pathog Dis* **71**: 292–301.

Arias-Barrau, E., Olivera, E.R., Luengo, J.M., Fernandez, C., Galan, B., Garcia, J.L., *et al*. (2004) The homogentisate pathway: a central catabolic pathway involved in the degradation of L-phenylalanine, L-tyrosine, and 3-hydroxyphenylacetate in *Pseudomonas putida*. *J Bacteriol* **186**: 5062–5077.

Bernal, V., Sevilla, A., Cánovas, M., and Iborra, J.L. (2007) Production of L-carnitine by secondary metabolism of bacteria. *Microb Cell Fact* **6**: 31.

Bertani, G. (1951) Studies on lysogenesis. I. The mode of phage liberation by lysogenic *Escherichia coli*. *J Bacteriol* **62**: 293–300.

Bolger, A.M., Lohse, M., and Usadel, B. (2014) Trimmomatic: a flexible trimmer for Illumina sequence data. *Bioinformatics* **30**: 2114-2120.

Bradford, M.M. (1976) A rapid and sensitive method for the quantitation of microgram quantities of protein utilizing the principle of protein-dye binding. *Anal Biochem* **72**: 248–254.

Breisch, J., Waclawska, I., and Averhoff, B. (2018) Identification and characterization of a carnitine transporter in *Acinetobacter baumannii*. *Microbiology* **8**: e00752.

Camarena, L., Bruno, V., Euskirchen, G., Poggio, S., and Snyder, M. (2010) Molecular mechanisms of ethanol-induced pathogenesis revealed by RNA-sequencing. *PLoS Pathog* **6**: e1000834.

Crouzet, P., and Otten, L. (1995) Sequence and mutational analysis of a tartrate utilization operon from *Agrobacterium vitis*. *J Bacteriol* **177**: 6518–6526.

Dean, A.M., and Dvorak, L. (1995) The role of glutamate 87 in the kinetic mechanism of *Thermus thermophilus* isopropylmalate dehydrogenase. *Protein Sci* **4**: 2156–2167.

Dijkshoorn, L., Nemec, A., and Seifert, H. (2007) An increasing threat in hospitals: multidrug-resistant *Acinetobacter baumannii*. *Nat Rev Microbiol* **5**: 939–951.

Dijkshoorn, L., Van Vianen, W., Degener, J.E., and Michel, M.F. (1987) Typing of *Acinetobacter calcoaceticus* strains isolated from hospital patients by cell envelope protein profiles. *Epidemiol Infect* **99**: 659–667.

Ditullio, D., Anderson, D., Chen, C.S., and Sih, C.J. (1994) L-carnitine *via* enzyme-catalyzed oxidative kinetic resolution. *Bioorg Med Chem* **2**: 415–420.

Djahanschiri, B., Di Venanzio, G., Distel, J.S., Breisch, J., Dieckmann, M.A., Goesmann, A., *et al*. (2022) Evolutionarily stable gene clusters shed light on the common grounds of pathogenicity in the Acinetobacter calcoaceticus-baumannii complex. *PLoS Genet* (in press).

Engel, A.G., and Rebouche, C.J. (1984) Carnitine metabolism and inborn errors. *J Inherit Metab Dis* **7**: 38–43.

Ezezika, O.C., Haddad, S., Neidle, E.L., and Momany, C. (2007) Oligomerization of BenM, a Lys R-type transcriptional regulator: structural basis for the aggregation of proteins in this family. *Acta Crystallogr Sect F Struct Biol Cryst Commun* **63**: 361–368.

Fiester, S.E., and Actis, L.A. (2013) Stress responses in the opportunistic pathogen *Acinetobacter baumannii*. *Future Microbiol* **8**: 353–365.

Giffhorn, F., and Kuhn, A. (1983) Purification and characterization of a bifunctional L-(+)-tartrate dehydrogenase-D-(-+)-malate dehydrogenase (decarboxylating) from *Rhodopseudomonas sphaeroides* Y. *J Bacteriol* **155**: 281–290.

Harding, C.M., Hennon, S.W., and Feldman, M.F. (2018) Uncovering the mechanisms of *Acinetobacter baumannii* virulence. *Nat Rev Microbiol* **16**: 91–102.

Hubloher, J.J., Zeidler, S., Lamosa, P., Santos, H., Averhoff, B., and Müller, V. (2020) Trehalose-6-phosphate-mediated phenotypic change in *Acinetobacter baumannii*. *Environ Microbiol* **22**: 5156–5166.

Keller, G.H., and Ladda, R.L. (1979) Quantitation of phosphatidylcholine secretion in lung slices and primary cultures of rat lung cells. *Proc Natl Acad Sci U S A* **76**: 4102–4106.

Kleber, H.P., Seim, H., Aurich, H., and Strack, E. (1977) Verwertung von Trimethylammoniumverbindungen durch *Acinetobacter calcoaceticus*. *Arch Microbiol* **112**: 201–206.

Koeth, R.A., Wang, Z., Levison, B.S., Buffa, J.A., Org, E., Sheehy, B.T., *et al*. (2013) Intestinal microbiota metabolism of L-carnitine, a nutrient in red meat, promotes atherosclerosis. *Nat Med* **19**: 576–585.

König, P., Averhoff, B., and Müller, V. (2021) K^+ and its role in virulence of *Acinetobacter baumannii*. *Int J Med Microbiol* **311**: 151516.

Laemmli, U.K. (1970) Cleavage of structural proteins during the assembly of the head of bacteriophage T4. *Nature* **227**: 680-685.

Lisa, T.A., Lucchesi, G.I., and Domenech, C.E. (1994) Pathogenicity of *Pseudomonas aeruginosa* and its relationship to the choline metabolism through the action of cholinesterase, acid phosphatase, and phospholipase C. *Curr Microbiol* **29**: 193–199.

Lochowska, A., Iwanicka-Nowicka, R., Plochocka, D., and Hryniewicz, M.M. (2001) Functional dissection of the Lys R-type Cys B transcriptional regulator. Regions important for DNA binding, inducer response, oligomerization, and positive control. *J Biol Chem* **276**: 2098–2107.

Love, M.I., Huber, W., and Anders, S. (2014) Moderated estimation of fold change and dispersion for RNA-seq data with DESeq2. *Genome Biol* **15**: 550.

Lu, S., Wang, J., Chitsaz, F., Derbyshire, M.K., Geer, R.C., Gonzales, N.R., *et al*. (2020) CDD/SPARCLE: the conserved domain database in 2020. *Nucleic Acids Res* **48**: D265–D268.

Lucchesi, G.I., Lisa, T.A., Casale, C.H., and Domenech, C. E. (1995) Carnitine resembles choline in the induction of cholinesterase, acid phosphatase, and phospholipase C and in its action as an osmoprotectant in *Pseudomonas aeruginosa*. *Curr Microbiol* **30**: 55–60.

Lukas, H., Reimann, J., Kim, O.B., Grimpo, J., and Unden, G. (2010) Regulation of aerobic and anaerobic D-malate metabolism of *Escherichia coli* by the Lys R-type regulator Dml R (YeaT). *J Bacteriol* **192**: 2503–2511.

Maddocks, S.E., and Oyston, P.C.F. (2008) Structure and function of the LysR-type transcriptional regulator (LTTR) family proteins. *Microbiology* **154**: 3609–3623.

Martínez-Luque, M., Castillo, F., and Blasco, R. (2001) Assimilation of D-malate by *Rhodobacter capsulatus* E1F1. *Curr Microbiol* **43**: 154–157.

Massmig, M., Reijerse, E., Krausze, J., Laurich, C., Lubitz, W., Jahn, D., and Moser, J. (2020) Carnitine metabolism in the human gut: characterization of the two-component carnitine monooxygenase CntAB from *Acinetobacter baumannii*. *J Biol Chem* **295**: 13065–13078.

McCann, M.R., George De la Rosa, M.V., Rosania, G.R., and Stringer, K.A. (2021) L-Carnitine and acylcarnitines: mitochondrial biomarkers for precision medicine. *Metabolites* **11**: 51.

Meadows, J.A., and Wargo, M.J. (2015) Carnitine in bacterial physiology and metabolism. *Microbiology* **161**: 1161–1174.

Miao, J., Ling, A.V., Manthena, P.V., Gearing, M.E., Graham, M.J., Crooke, R.M., *et al*. (2015) Flavin-containing monooxygenase 3 as a potential player in diabetes-associated atherosclerosis. *Nat Commun* **6**: 6498.

Miyazaki, K., Kakinuma, K., Terasawa, H., and Oshima, T. (1993) Kinetic analysis on the substrate specificity of 3-isopropylmalate dehydrogenase. *FEBS Lett* **332**: 35–36.

Patro, R., Duggal, G., Love, M.I., Irizarry, R.A., and Kingsford, C. (2017) Salmon provides fast and bias-aware quantification of transcript expression. *Nat Methods* **14**: 417–419.

Peleg, A.Y., Seifert, H., and Paterson, D.L. (2008) *Acinetobacter baumannii*: emergence of a successful pathogen. *Clin Microbiol Rev* **21**: 538–582.

R Core Team. (2020) *R: A Language and Environment for Statistical Computing.* Vienna: R Foundation for Statistical Computing.

Soneson, C., Love, M.I., and Robinson, M.D. (2015) Differential analyses for RNA-seq: transcript-level estimates improve gene-level inferences. *F1000Res* **4**: 1521.

Stahl, J., Bergmann, H., Göttig, S., Ebersberger, I., and Averhoff, B. (2015) *Acinetobacter baumannii* virulence is

mediated by the concerted action of three phospholipases D. *PLoS One* **10**: e0138360.

Stokke, R., Madern, D., Fedøy, A.E., Karlsen, S., Birkeland, N.K., and Steen, I.H. (2007) Biochemical characterization of isocitrate dehydrogenase from *Methylococcus capsulatus* reveals a unique NAD^+-dependent homotetrameric enzyme. *Arch Microbiol* **187**: 361–370.

Tipton, P.A., and Peisach, J. (1990) Characterization of the multiple catalytic activities of tartrate dehydrogenase. *Biochemistry* **29**: 1749–1756.

Towner, K.J. (2009) *Acinetobacter*: an old friend, but a new enemy. *J Hosp Infect* **73**: 355–363.

Villegas, M.V., and Hartstein, A.I. (2003) *Acinetobacter* outbreaks, 1977-2000. *Infect Control Hosp Epidemiol* **24**: 284–295.

Vorobieva, A.A., Khan, M.S., and Soumillion, P. (2014) *Escherichia coli* D-malate dehydrogenase, a generalist enzyme active in the leucine biosynthesis pathway. *J Biol Chem* **289**: 29086–29096.

Wargo, M.J., Ho, T.C., Gross, M.J., Whittaker, L.A., and Hogan, D.A. (2009) Gbd R regulates *Pseudomonas aeruginosa plc H* and *pch P* transcription in response to choline catabolites. *Infect Immun* **77**: 1103–1111.

Wargo, M.J., and Hogan, D.A. (2009) Identification of genes required for *Pseudomonas aeruginosa* carnitine catabolism. *Microbiology* **155**: 2411–2419.

Wendt, C., Dietze, B., Dietz, E., and Rüden, H. (1997) Survival of *Acinetobacter baumannii* on dry surfaces. *J Clin Microbiol* **35**: 1394–1397.

Zachowski, A. (1993) Phospholipids in animal eukaryotic membranes: transverse asymmetry and movement. *Biochem J* **294**: 1–14.

Zeidler, S., Hubloher, J., Schabacker, K., Lamosa, P., Santos, H., and Müller, V. (2017) Trehalose, a temperature- and salt-induced solute with implications in pathobiology of *Acinetobacter baumannii*. *Environ Microbiol* **19**: 5088–5099.

Zeidler, S., and Müller, V. (2019) Coping with low water activities and osmotic stress in *Acinetobacter baumannii*: significance, current status and perspectives. *Environ Microbiol* **21**: 2212–2230.

Zhu, A., Ibrahim, J.G., and Love, M.I. (2019) Heavy-tailed prior distributions for sequence count data: removing the noise and preserving large differences. *Bioinformatics* **35**: 2084–2092.

Zhu, Y., Jameson, E., Crosatti, M., Schäfer, H., Rajakumar, K., Bugg, T.D., and Chen, Y. (2014) Carnitine metabolism to trimethylamine by an unusual Rieske-type oxygenase from human microbiota. *Proc Natl Acad Sci U S A* **111**: 4268–4273.

Supporting Information

Additional Supporting Information may be found in the online version of this article at the publisher's web-site:

Appendix S1. Supporting information.